GeoPlanning
Journal of Geomatics and Planning

Geoplanning: Journal of Geomatics and Planning, Vol. 11, No. 2, 2024, 189-204

e-ISSN: 2355-6544

Received: 03 September 2024;
Revised: 29 October 2024;
Accepted: 29 November 2024;
Available Online: 30 November 2024;
Published: 04 December 2024.

Keywords:
Natural Hazard, Flood, Risk, GIS, Solo River Watershed

*Corresponding author(s)
email: jumadi@ums.ac.id

Original Research Open access

Utilizing Open Access Spatial Data for Flood Risk Mapping: A Case Study in the Upper Solo Watershed

J. Jumadi[1,2*], D. Danardono[1,2], Kuswaji D. Priyono[1,2], Efri Roziaty[2,3], Heni Masruroh[4], Arif Rohman[5], Choirul Amin[1], Hamim Zaky Hadibasyir[1], Vidya N. Fikriyah[1,6], Muhammad Nawaz[7], Farha Sattar[8], Aynaz Lotfata[9]

1 *Faculty of Geography, Universitas Muhammadiyah Surakarta, Surakarta 57162, Indonesia*
2 *Center of Environmental Studies, Universitas Muhammadiyah Surakarta, Surakarta 57162, Indonesia*
3 *Faculty of Education, Universitas Muhammadiyah Surakarta, Surakarta 57162, Indonesia;*
4 *Department of Geography, Malang State University, Malang, Indonesia*
5 *Department of Geomatic, ITERA, Lampung, Indonesia*
6 *Faculty of Geo-information Science and Earth Observation (ITC), University of Twente, Drienerlolaan 5, 7522 NB Enschede, The Netherland*
7 *Department of Geography, National University of Singapore, 1 Arts Link, Block AS2, Singapore 117570*
8 *Faculty of Arts & Society, Education & Enabling, Charles Darwin University, Ellengowan Drive, Casuarina NT 0810, Australia*
9 *University of California, Davis, USA*

DOI: 10.14710/geoplanning.11.2.189-204

Abstract

Indonesia is experiencing a rise in natural disasters due to its geographical position within a tropical region, with the Upper Solo River watershed exhibiting a heightened risk of flooding. This region has already suffered numerous floods due to excessive precipitation and insufficient drainage. Susceptibility, hazard, and risk studies have been conducted to investigate this phenomenon but have been limited to specific regions within the catchment area. This study aims to construct a GIS-based flood risk model using Open-Access Spatial Data (OASD) based on diverse physical characteristics, urbanization levels, and population. We used several OASD, including SRTM, Sentinel 2 MSI, GPM v6, NASA-USDA Enhanced SMAP Global Soil Moisture Data, GHS-SMOD R2023A - Global Human Settlement Layers, and GHSL: Global Population Surfaces 1975-2030 (P2023A). The model integrates the risk parameters to identify flood risk using a weighted overlay in ArcGIS. The results demonstrate spatial heterogeneity in flood risk throughout the watershed. The result also reveals that Surakarta City, with a high proportion of its area in the 'High' (57.3%) and 'Very High' (29.54%) risk categories, is at the highest risk of flooding within the watershed. The study enhances understanding of this topic by comprehensively evaluating flood hazards, vulnerabilities, and risks. It highlights the significance of utilizing low-cost OASD to improve flood preparedness and response strategies.

Copyright © 2024 by Authors,
Published by Universitas Diponegoro Publishing Group.
This open access article is distributed under a
Creative Commons Attribution 4.0 International license

1. Introduction

The frequency of natural catastrophes seems to rise due to natural phenomena and human activities, leading to significant human casualties, property damage, and material losses. Human activities, such as deforestation, land clearance on mountain slopes, and cultivation of steeply sloping lands, have the potential to give rise to natural disasters. Due to its geographical positioning within a region characterized by dynamic

tectonic activity and volcanic activity resulting from the convergence of three tectonic plates, namely the Indian-Australian Plate, the Pacific Plate, and the Eurasia Plate, Indonesia is prone to disasters (Jumadi et al., 2016). Floods in the country are significant natural disasters that can have disastrous consequences (Susetyo, 2008), with Indonesia having the highest incidence of flood disasters in Southeast Asian countries from 1980 to 2018 (Samphantharak, 2019).

The origin of flood events, a phenomenon experienced in the region for many years, can be traced back. Heavy rains combined with depreciative drainage are one of the main causes of flooding in the area. The Upper Solo River watershed's previous flood histories are represented by historical statistics that show many major floods. Especially in 1966, 2007, 2009, and 2010, the region suffered from severe flooding because of heavy rain (Damayanti, 2011; Fathimah & Dahroni, 2014; Gunawan, 2009), with these particular events being the most serious in recorded history. Heavy rains, therefore, can devastate infrastructure, such as roads and bridges, and lead to the loss of life. The region has undergone periodic flooding, mainly due to heavy precipitation and inadequate drainage, since the 2007 flood, which was by far the worst in fifty years and submerged 11,500 homes (Zein, 2010). Subsequently, the municipal authorities have begun this preparation coupled with upgrades to the drainage infrastructure within the area, with the intention of reducing flooding. However, despite such continuing attempts, the Upper Solo River watershed remains susceptible to flooding, especially during the rainy season. In recent years, intense and extreme weather conditions have increased; as a result, the area has been significantly affected in the form of a higher frequency of flooding. For this reason, it is vital to manage and develop disaster-fighting measures to keep the impact of the floods on the residents in the region to a minimum.

Floods are natural calamities that must be prevented entirely. Complex hydrological, geological, and geomorphological circumstances, combined with deforestation and urbanization, contribute to floods, resulting in substantial social, economic, and environmental consequences (Amin et al., 2020; Curebal et al., 2016; Komolafe et al., 2020; Mukherjee & Singh, 2020; Mustikaningrum et al., 2023; Nada et al., 2023; Sejati et al., 2023; Purwitaningsih et al., 2020; Saputra et al., 2022; Skilodimou et al., 2019). Factors like deforestation and urbanization disrupt soil absorption, resulting in unsuitable surfaces and causing further damage. As a consequence, rainwater collected from impervious surfaces accelerates the velocity and height of the intense flows that exacerbate flood events. Urbanization and land use alterations can modify the built environment, impacting hydrological systems and altering river flow rates, hence heightening the risk of catastrophic flooding in specific sensitive areas (Chagas et al., 2022). Flooding constitutes a disaster as it adversely affects society, the economy, and the environment (Komolafe et al., 2020; Mukherjee & Singh, 2020; Skilodimou et al., 2019). Floods result in fatalities, population displacement, infrastructure damage, agricultural and livestock losses, disease transmission, and water supply contamination (Rincón et al., 2018). Consequently, it is essential to provide flood-related information to mitigate risks.

A multitude of studies has been undertaken concerning flood analysis utilizing Geographic Information Systems (GIS) and remote sensing technologies (Elkhrachy, 2015; Greene & Cruise, 1995; Islam & Sado, 2000; Jumadi et al., 2024; Ozkan & Tarhan, 2016; Paudyal, 1996; Tehrany et al., 2017).Various methodologies have been employed, including the spatial multi-criteria method (Chen et al., 2012; Zhou et al., 2021), cellular automata (CA) (Ghimire et al., 2013), a one-dimensional hydraulic drainage network model (Jamali et al., 2018), and Analytical Hierarchical Processes (AHP) (Negese et al., 2022; Sarmah et al., 2020). Nonetheless, research employing comprehensive open access spatial data for all variables is still limited. Recent research has persistently utilized non-open access data sources for particular variables such as soil type (Diriba et al., 2024; Osman & Das, 2023); rainfall (Rana et al., 2024); flood depth (Ayenew & Kebede, 2023); flood-prone areas (Li et al., 2024); and geology (Osman & Das, 2023). Geographic Information Systems (GIS) and remote sensing offer effective frameworks for assessing flood hazards; nonetheless, the use of proprietary or restricted data sets may hinder accessibility and repeatability in this domain. In contrast, unrestricted open-access geographical data may serve as a more economical and transparent alternative to democratize flood risk analysis in low- and middle-income nations.

Nevertheless, the degree to which open-access data can be included into flood risk studies necessitates further investigation in this underutilized domain; hence, traditional data sources should be employed, since they have been previously validated in other contexts. Consequently, the integration of GIS and Remote Sensing (RS) data with additional databases, facilitated by contemporary technical improvements, enables the identification, monitoring, and assessment of flood disasters (Biswajeet & Mardiana, 2009; Haq et al., 2012; Pradhan et al., 2009). The initial stage in comprehensively comprehending all aspects leading to flooding may entail the integration of diverse datasets into a broader framework for formulating flood control plans. Various strategies have been utilized to tackle the flooding issue, including a flood hazard mapping tool that identifies regions at elevated risk of flooding. This study aims to construct a GIS-based flood risk model using Open-Access Spatial Data (OASD) based on diverse physical characteristics, urbanization levels, and population. This study utilized physical characteristics and urbanization variables as stakeholders aim to produce a flood risk model for the upper reaches of the Solo River by integrating GIS and RS data in its construction process.

In order to achieve the objective, the subsequent sections of this work are structured as follows. The following section presents a comprehensive overview of the methodologies, encompassing data collection techniques, descriptions of the parameters utilized for risk analysis, and the study framework employed. The subsequent section expounds on the outcomes and analysis, discussing the perils associated with flooding; vulnerability influenced by the degree of urban development, the associated risks; and the comprehensive findings. The concluding section presents a summary of the findings.

2. Data and Methods

2.1. Study Area

The research was conducted in the upper part of the Bengawan Solo watershed (Figure 1), located between 110°13'7.16" -110°26 '57.10" East and 7°26 '33.15" -8°6 '13.81" South. The watershed is the largest catchment area on Java Island, Indonesia, covering a total area of 16,100 km2, and it plays a significant role in providing water for the daily needs and agriculture of those living in the area. It comprises three sub-watersheds: the upper Bengawan Solo, Kali Madiun, and the lower Bengawan Solo. The upper Bengawan Solo area covers approximately 6,000 km². The topographic condition of the study area is varied; it is dominantly flat but with relatively undulating terrain in the northeast and northwest parts of the watershed close to the mountains. Upper Bengawan Solo provides water from Mount Merapi and Mount Merbabu in the western part of the Bengawan Solo River and from Mount Lawu in the eastern region.

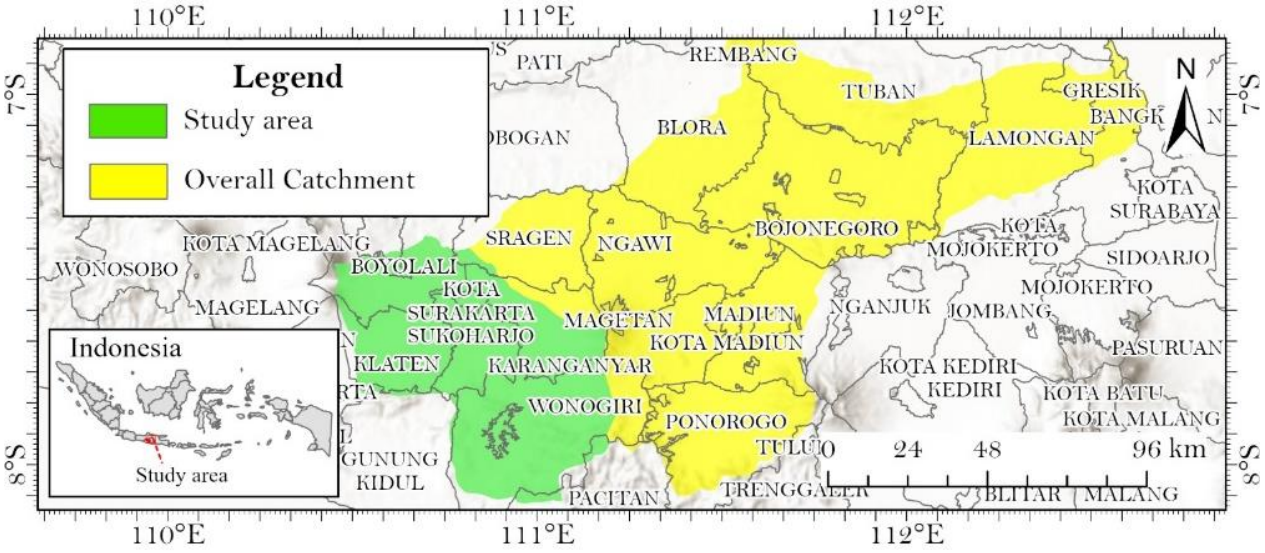

Figure 1. The Study Area

2.2. Datasets

The study used several spatial datasets to develop the risk level model. First, shuttle radar topographic mission (SRTM) data with 30m resolution was acquired as the digital elevation model. Land cover and land use information was then interpreted from remote sensing image Sentinel-2 (10 m spatial resolution). Global precipitation measurement (GPM) data were utilized to obtain rainfall information, while soil moisture active passive (SMAP) data were used to establish the soil moisture condition of the study area. GHSL and GHS-SMOD R2023A datasets are also used in this study. These datasets aid in analyzing human settlement patterns, density, and spatial changes, enhancing the demographic characteristics of the study area. All dataset characteristics and their sources are provided in Table 1.

Table 1. Flood Risk Parameter Data Sources

No	Data	Description	Source	Derived Data
1.	DEM	Shuttle Radar Topography Mission (SRTM).	USGS (Earth Resources Observation and Science (EROS) Center, 2017)	El, Sl, FA, DR, Cu, DD, TWI
2.	Images	Sentinel 2 Multispectral Instrument	ESA (ESA, 2023)	LULC, NDVI
3.	Rainfall data	Global Precipitation Measurement (GPM) v6.	NASA (NASA, 2019)	RF
4.	Soil moisture data	NASA-USDA Enhanced SMAP Global Soil Moisture Data.	NASA (Entekhabi et al., 2010)	SM
5.	Level of urbanization	GHS-SMOD R2023A - Global Human Settlement Layers.	European Commission, Joint Research Centre (JRC) (Earth Engine Data Catalog, 2023; Pesaresi & Politis, 2023; Santillan & Heipke, 2023; Schiavina et al., 2023)	DoU
6.	Population	GHSL: Global population surfaces 1975-2030 (P2023A)	Earth Engine Data Catalog (Google Earth Engine Data Catalog, 2023)	Pop

Note: El – elevation, Sl – slope, FA – flow accumulation, DR – distance to rivers, Cu – curvature, DD – drainage density, TWI – topographic wetness index, LULC – land use land cover, NDVI – normalized difference vegetation index, RF – rainfall, SM – soil moisture, URSD – Level of Urbanization, Pop - Population.

2.3. Research Framework

The study area flood-risk levels were determined using the general risk function (Equation 1) (Sar et al., 2015; UNISDR, 2004). The study was separated into three main sections: flood hazard, vulnerability and risk analysis (Figure 2). Flood hazard was determined by weighted overlay operation of certain physical parameters related to flood occurrences (Table 2). Similarly, vulnerability was indicated by using weighted overlay by parameters related to population and level of urbanization (Table 3). Finally, risk was determined by multiplying hazard by vulnerability (Samarasinghea et al., 2010).

$$R = H \times V \ldots\ldots\ldots\ldots\ldots \textit{(Equation. 1)}$$

Various parameters are used to define flood hazards, such as El, Sl, FA, DR, Cu, DD, TWI, LULC, NDVI, RF, and SM are modified from Negese et al. (2022) and Purwanto et al. (2023). Low-lying locations exhibit significant water accumulation, heightening flooding threats due to markedly reduced flow velocity in the flat portions of the terrain. The proximity of a river increases the likelihood of floods. Areas at lower elevations near rivers are more susceptible to flooding due to elevated discharge rates and reduced water velocity. Flood events are precipitated by flow accumulation and drainage density; elevated levels of flow accumulation and drainage density augment the probability of flooding. Consequently, Land Use and Land Cover (LULC) are critical to assessing flood risk, as areas with high vegetation density demonstrate reduced susceptibility due to delayed water movement and enhanced infiltration rates. Consequently, soil qualities are crucial; fine soils are recognized for accelerating surface runoff while diminishing permeability, thereby heightening the likelihood of inundation.

Table 2. Flood Hazard Indicators

No	Factor	Classification	Degree of Flood Hazard	Score	Weight (%)
1.	Slope (Sl) (Degree)	> 45	Very Low	1	15
		25-45	Low	2	
		15-25	Moderate	3	
		8-15	High	4	
		0-8	Very High	5	
2.	Rainfall (Rf) (mm)	1,696-1,728	Very Low	1	11
		1,728-1,761	Low	2	
		1,761-1,793	Moderate	3	
		1,793-1,825	High	4	
		> 1,825	Very High	5	
3.	Drainage Density (DD) (km/km2)	0-0.372	Very Low	1	8
		0.372-0.754	Low	2	
		0.754-1.106	Moderate	3	
		1.106-1.519	High	4	
		>1.519	Very High	5	
4.	Soil Moisture (SM)(m^3/m^3)	15.4-16.14	Very Low	2	4
		16.14-16.68	Low		
		16.68-17.42	Moderate	3	
		17.42-18.49	High	4	
		18.49-20.53	Very High	5	
5.	Land Use/ Land Cover (LULC)	Dense Vegetation	Very Low	1	7
		Bare land	Low	2	
		Open Mining	Moderate	3	
		Cropland	High	4	
		Built-up area	Very High	5	
6.	Elevation (El) (m amsl)	558.8 - 697	Very Low	1	18
		420.6 - 558.8	Low	2	
		282.4 - 420.6	Moderate	3	
		144.2 - 282.4	High	4	
		6 - 144.2	Very High	5	
7.	Distance to river (DR) (m)	0.372 - 1.2976	Very High	1	11
		1.2976 - 2.2232	High	2	
		2.2232 - 3.1488	Moderate	3	
		3.1488 - 4.0744	Low	4	
		4.0744 - 5	Very Low	5	
8.	NDVI	– 0.16–0.29	Very Low	1	3
		0.29–0.38	Low	2	
		0.38–0.45	Moderate	3	
		0.45–0.51	High	4	
		0.51–0.59	Very High	5	
9.	Curvature (Ct)	Convex (positive)	Moderate	1	2
		Concave (negative)	High	2	
		Flat	Very High	3	
10.	Flow Accumulation (FA)	< 250	Very Low	1	15
		250–2195	Low	2	
		2195–3415	High	4	
		3415–15,125	Very High	5	
11.	Topographic Wetness Index (TWI)	2.48–5.91	Very Low	1	6
		5.91–8.09	Low	2	
		8.09–10.18	Moderate	3	
		10.18–12.63	High	4	
		12.63–22.77	Very High	5	

Additional factors encompass NDVI and curvature, which further assessing an area's vulnerability to flooding events. Regions with greater vegetation cover exhibit prolonged precipitation runoff, whereas flat plain areas are especially susceptible to flooding. Finally, precipitation and TWI indices were utilized, revealing that significant rainfall provided substantial water, which, when combined with TWI, indicated regions likely to possess saturated soils prone to flooding. Curvature is a fundamental characteristic of the Earth's surface, articulated by geomorphometric techniques. In this instance, it may serve as an effective instrument for flood

management because to its correlation with water distribution and concentration (Faisal & Hayakawa, 2023; Sofia, 2020; Xiong et al., 2022).

GIS-based flood hazard maps were generated using ArcGIS overlays of flood components assigned specific weights. Flood formation occurs due to eleven primary parameters: land slope (Sl), elevation (El), flow accumulation (FA), rainfall (Rf), drainage density (DD), distance to rivers (DR), topographic wetness index (TWI), normalized difference vegetation index (NDVI), land use land cover (LULC), soil type (ST), and curvature of water surface (Cu)—consequently, raster data formats generated spatially refined information regarding these 11 parameters. Low-lying areas exhibit significant water accumulation, heightening the risk of floods due to markedly reduced flow velocity in the flat portions of the terrain. The proximity of rivers increases the likelihood of floods. Areas at lower elevations near rivers are more susceptible to flooding due to elevated discharge rates and reduced water velocity. Flood events are precipitated by flow buildup and drainage density; elevated levels of both factors augment the probability of flooding. Consequently, Land Use and Land Cover (LULC) are critical to assessing flood risk, as areas with high vegetation density demonstrate reduced susceptibility due to delayed water movement and enhanced infiltration rates. Consequently, soil properties emerge as a significant factor: Fine soils are recognized for accelerating surface runoff while reducing permeability, heightening the likelihood of inundation.

Additional criteria encompass NDVI and curvature, further influencing an area's vulnerability to flooding events. Regions with greater vegetation cover experience prolonged rainwater runoff, whereas flat land areas are especially susceptible to flooding. Finally, precipitation and TWI indices were utilized, as significant rainfall provided additional water, which, when combined with TWI, indicated regions likely to possess saturated soils susceptible to flooding. Curvature is a fundamental characteristic of the Earth's surface, articulated by geomorphometric methods. In this context, it may serve as an effective instrument for flood management because to its correlation with water distribution and concentration (Faisal & Hayakawa, 2023; Sofia, 2020; Xiong et al., 2022). GIS-based flood hazard maps were generated using ArcGIS overlays of flood components assigned specific weights. Flood formation occurs due to eleven primary parameters: land slope (Sl), elevation (El), flow accumulation (FA), rainfall (Rf), drainage density (DD), distance to rivers (DR), topographic wetness index (TWI), normalized difference vegetation index (NDVI), land use land cover (LULC), soil type (ST), and curvature of water surface (Cu). Consequently, raster data formats were employed to generate spatially refined information regarding these 11 parameters.

Table 3. Vulnerability Indicators

No.	Factor	Classification	Degree of Vulnerability	Score	Weight (%)
1.	Population	0 - 12	Very Low	1	50
		13 - 37	Low	2	
		38 - 75	Moderate	3	
		76 - 127	High	4	
		128 - 290	Very High	5	
2.	Degree of urbanization	Water	Unclassified	0	50
		Very low density rural	Very Low	1	
		Low density rural	Low	2	
		Rural cluster	Low	2	
		Suburban or peri-urban	Moderate	3	
		Semi-dense urban cluster	High	4	
		Dense urban cluster	High	4	
		Urban center	Very high	5	

In addition, we quantified vulnerability based on the density of inhabitants. The higher the density, the higher the vulnerability. The GHS-SMOD R2023A dataset was used to provide this data. This is a spatial dataset that delineates the distribution and evolution of human settlements across the globe, tracking changes from 1975 through to 2030 in five-year increments. The dataset is instrumental in evaluating the susceptibility of various settlement types, highlighting an increased vulnerability in more densely populated areas (Melchiorri, 2022). The 2023A release of the Global Human Settlement Layer GHS-SMOD settlement segments were classified

into eight distinct types (Earth Engine Data Catalog, 2023; European Commission, 2023) (Table 3). For each type, a specific vulnerability level was determined, alongside a score that progressed from "Very Low" (1) for areas with very low density rural to "High" (5) for urban centers. This segmentation indicated a direct correlation between the compactness of the population of a settlement and its vulnerability to risks. In addition, the GHSL-derived global population surfaces from 1975-2030 (P2023A) classify flood vulnerability levels into five categories: Very Low (0-12), Low (13-37), Moderate (38-75), High (76-127), and Very High (128-290), based on population density. The impact of this analysis is significant, as it provides understanding of vulnerability that can inform more effective flood risk management. By leveraging this data, policymakers and emergency responders can prioritize resources and interventions in high-density areas, ultimately reducing the potential for loss of life and damage to property during flood events.

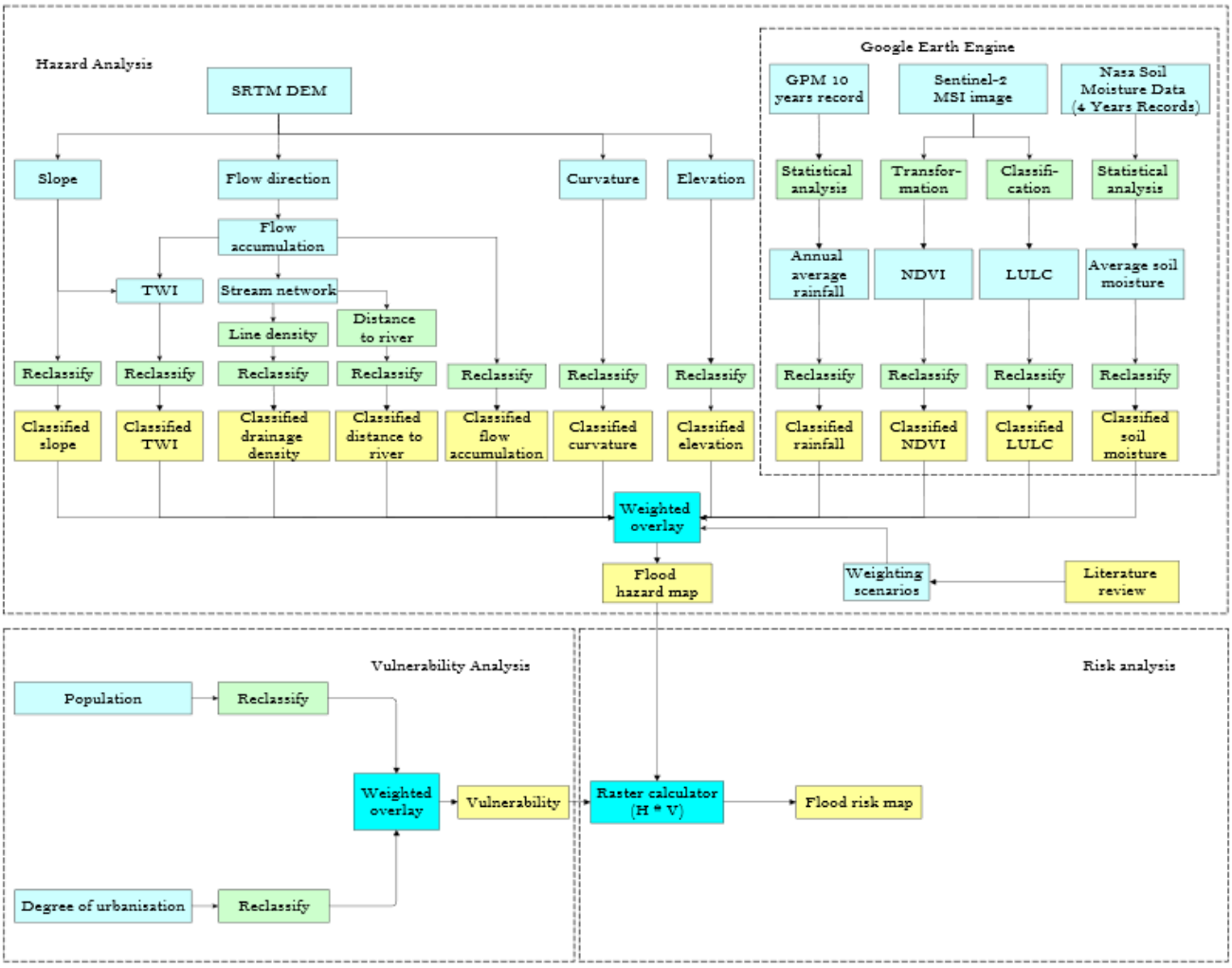

Figure 2. Research Framework

3. Result and Discussion

3.1 Flood Hazard Model

Figure 3 shows all the parameters used to define flood hazard, while the distribution of flood indicator classes in determining the hazard can be seen in Figure 4. Figure 5 shows the distribution of environmental and geographical factors across different flood hazard levels, providing quantitative insight into their impact on flood risk. Elevation is included in 57.64% of the "Very High" flood risk areas, with slopes in 49.15%. Distance to rivers is a critical factor in flood risk, with 42.24% of these areas near water bodies. Flow accumulation is high

in 99.81% of the "Very Low" risk areas, indicating efficient water dispersal mechanisms. The NDVI shows that vegetation cover decreases significantly in "Very High" risk areas, indicating the protective role of vegetation against flooding. Rainfall contributes differently across hazard levels, with a notable percentage of 28.27% in "Moderate" risk areas. Soil moisture is higher in lower-risk areas and decreases to 2.85% in "Very High" areas, highlighting the influence of soil water content on flood susceptibility. The Topographic Wetness Index (TWI) indicates potential water accumulation based on topography, with high levels in "Very Low" risk areas, but lower levels in "Very High" areas. Land use land cover (LULC) falls from 34.97% in "Very Low" risk areas to 7.76% in "Very High" ones, illustrating the impact of land cover and human land use on flood risk.

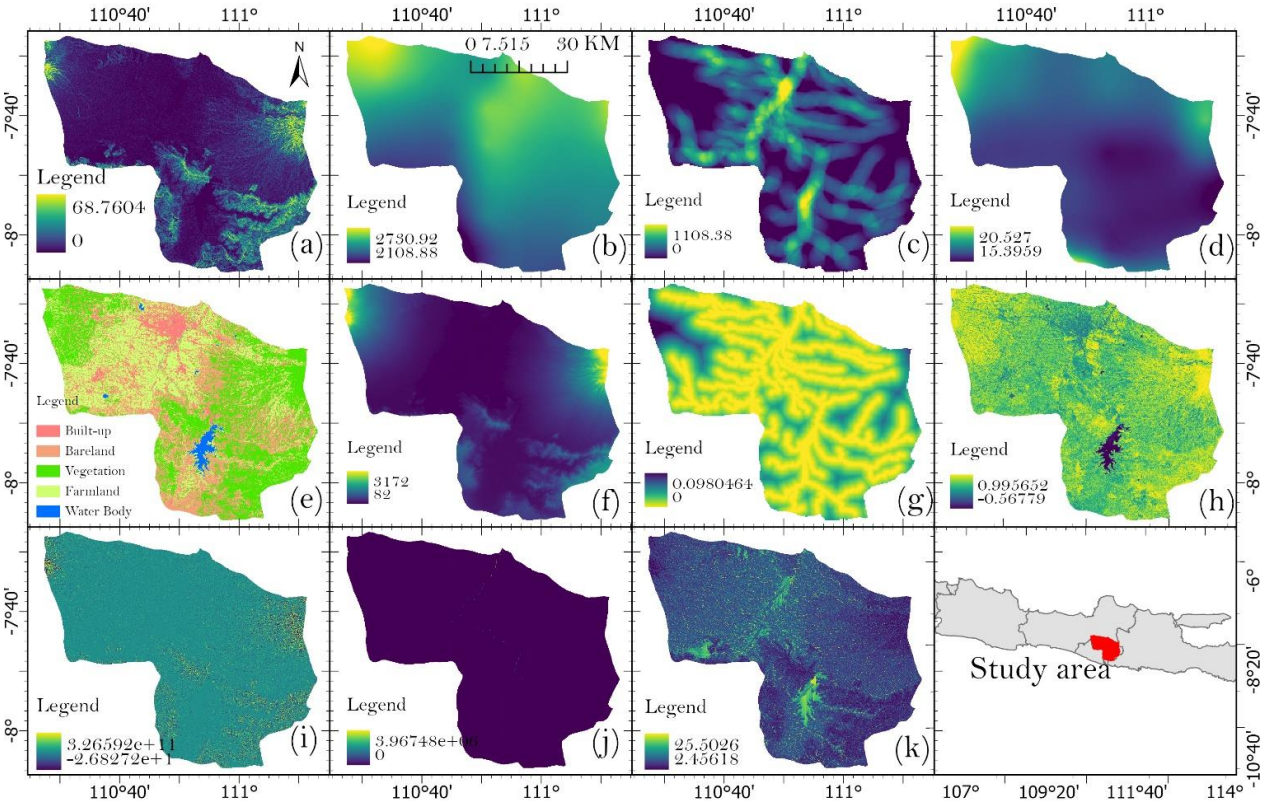

Figure 3. Flood Hazard Parameters. Note: (a) Sl, (b) RF, (c) DD, (d) SM, (e) LULC, (f) El, (g) DR, (h) NDVI, (i) Cu, (j) FA, (k) TWI

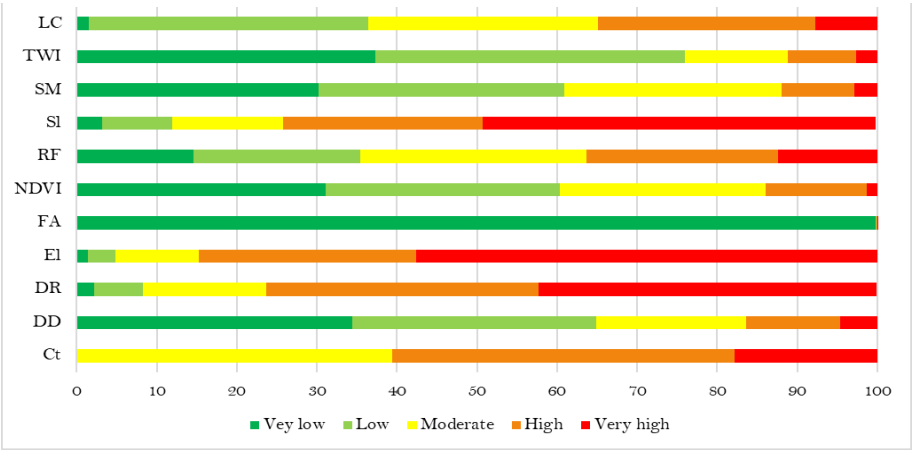

Figure 4. The Percentage of Hazard Classes based on the Parameters

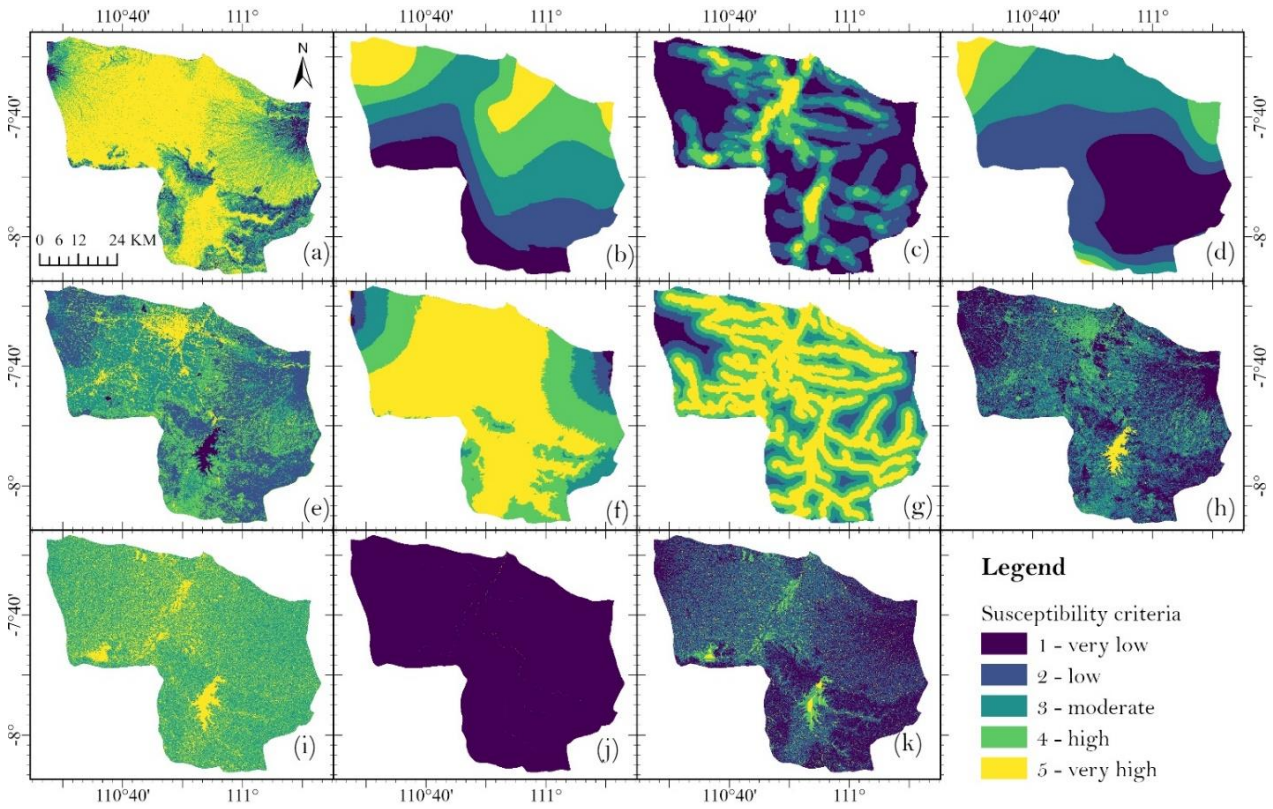

Figure 5. Reclassified Parameters. Note: (a) Sl, (b) RF, (c) DD, (d) SM, (e) LULC, (f) El, (g) DR, (h) NDVI, (i) Cu, (j) FA, (k) TWI

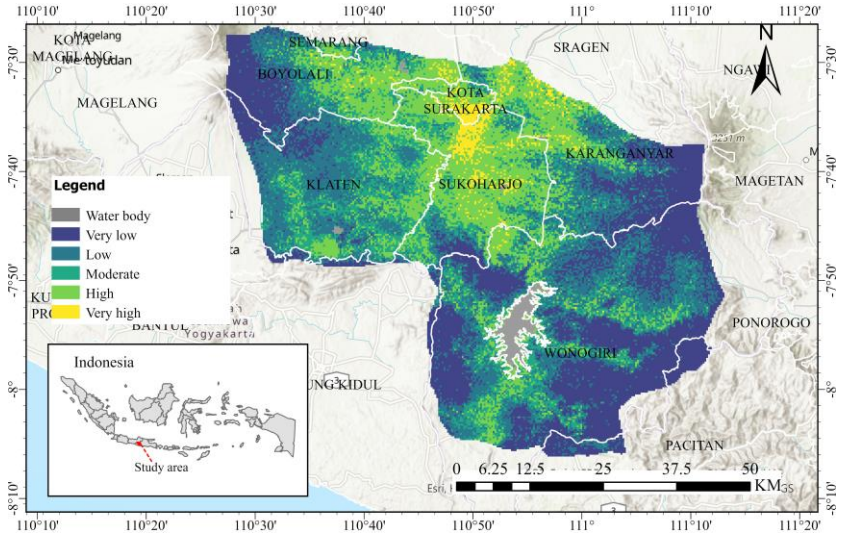

Figure 6. Flood Hazard Map

3.2 Flood Vulnerability

Figures 7 and 8 show the vulnerability indicators and their classification, respectively. Figure 7a shows the level of urbanization, which is classified into vulnerability levels from very low to very high in Figure 8a. Figure 7b shows population density, while Figure 8b shows the classification from very low to very high. Vulnerability distribution across the research area is shown in Figure 8. Based on weighted overlay, this map was produced as a composite from Figures 7b and 7c. The figure shows that urban areas are moderate to very

highly vulnerable. For example, Surakarta, Boyolali, Karanganyar, Klaten, and Sukoharjo exhibit a high presence within the 'Very High' classification and a significant one within the 'Very High' and 'Moderate' classifications.

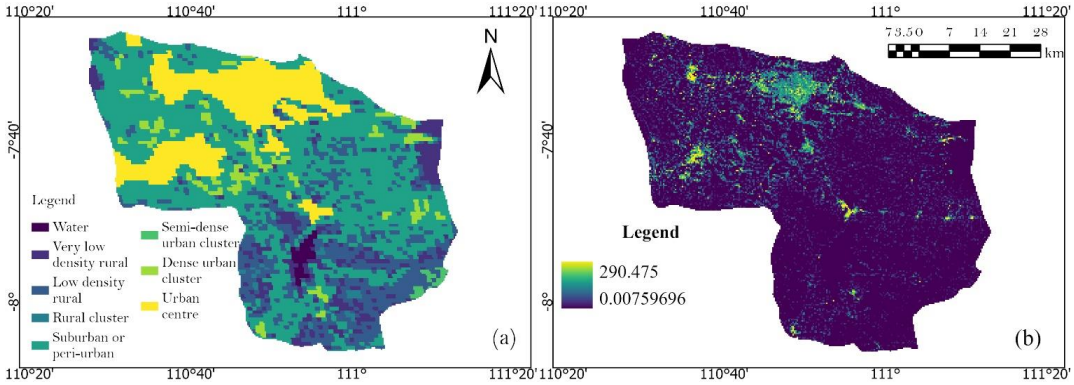

Figure 7. Vulnerability Factors and their Classification

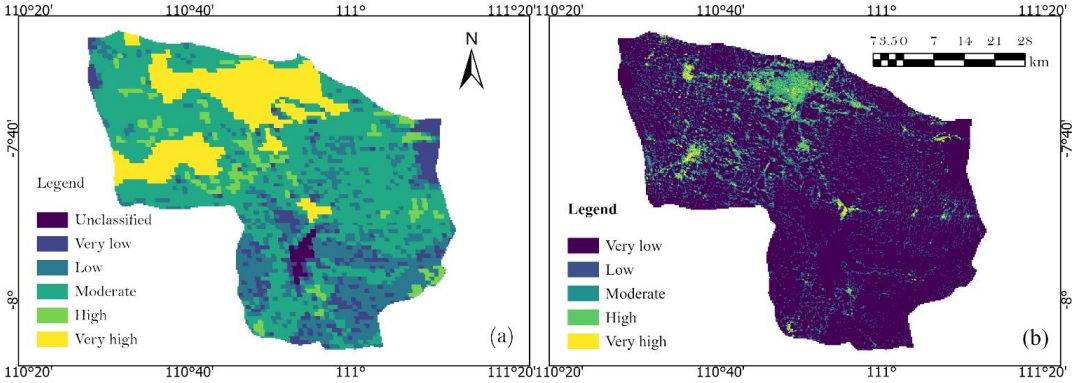

Figure 8. Vulnerability Factors and their Classification

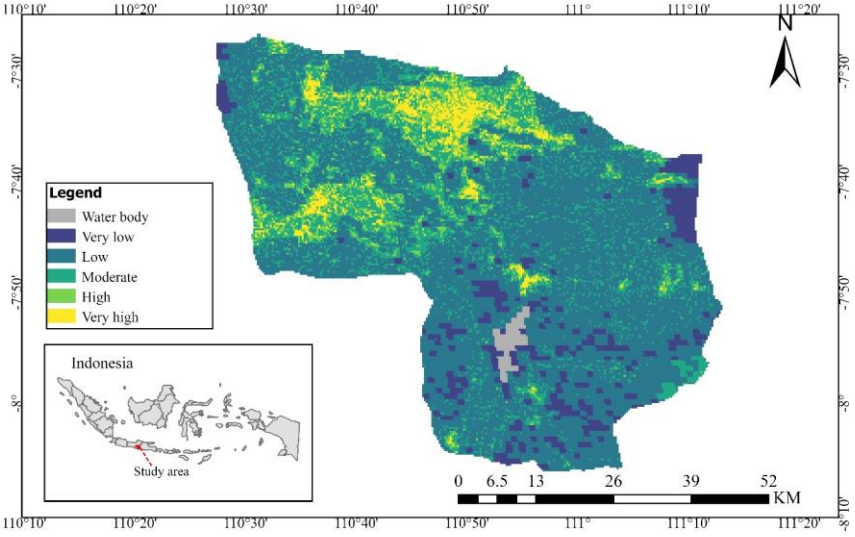

Figure 9. Vulnerability Class

3.3 Flood Risk Model

Table 4 indicates the flood risk in different cities and regencies within the watershed, whereas the spatial distribution is presented in Figure 9. Boyolali possesses a substantial proportion of land categorized as 'Moderate' risk, indicating a comprehensive approach to risk management. At the same time, Karanganyar exhibits diverse

risk levels, displaying an apparent propensity towards the 'Very Low' and 'High' classifications. The majority of the Kota Surakarta area, 57.3%, is classified as 'High' risk, with 29.54% classified as 'Very High,' highlighting the urgent need for comprehensive urban planning and measures to mitigate flood disasters.

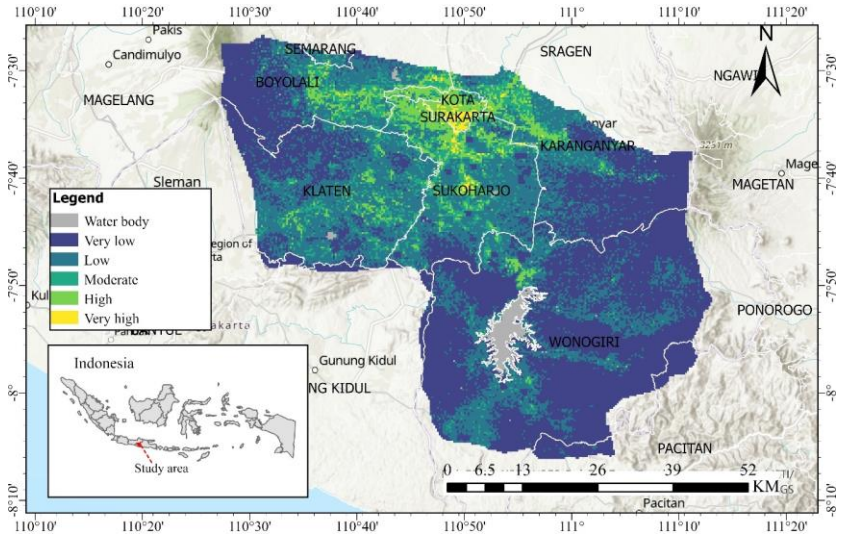

Figure 10. Flood Risk Map

Table 4. Area risk classes for each region.

Regency/City	Area Class												Total
	WB	%	VL	%	L	%	M	%	H	%	VH	%	
Boyolali	1.88	0.46	165.64	40.31	137.14	33.38	64.56	15.71	40.07	9.75	1.62	0.39	410.9
Gunung Kidul	0	0	34.28	91.35	3.23	8.6	0.02	0.05	0	0	0	0	37.52
Karanganyar	1.3	0.24	261.23	47.74	170.08	31.09	63.66	11.64	48.5	8.86	2.36	0.43	547.14
Klaten	1.88	0.29	191.88	29.75	346.11	53.66	79.84	12.38	25.27	3.92	0	0	644.99
Surakarta	0.21	0.45	0	0	1.93	4.21	3.89	8.5	26.24	57.3	13.53	29.54	45.79
Pacitan	0	0	66.71	97.21	1.91	2.79	0	0	0	0	0	0	68.62
Semarang	0	0	2.47	16.27	9.43	62.07	2.91	19.15	0.29	1.9	0.09	0.62	15.19
Sleman	0	0	4.13	99.17	0.03	0.83	0	0	0	0	0	0	4.17
Sragen	0	0	0	0	0	0	0.01	100	0	0	0	0	0.01
Sukoharjo	1.7	0.35	59.76	12.33	232.44	47.96	104.5	21.56	78.52	16.2	7.74	1.6	484.64
Wonogiri	54.15	3.92	983.05	71.1	365.41	26.43	30.5	2.21	9.22	0.67	0	0	1382.57

Note: WB – water body (sq km), VL – very low risk (sq km), L – low risk (sq km), M – moderate risk (sq km), H – high risk (sq km), VH – very high risk (sq km).

3.4 Discussion

The study has revealed varied flood vulnerabilities across the Upper Solo River watershed, highlighting regions of significant susceptibility and the necessity for customized flood mitigation strategies based on the data analysis. This analysis demonstrates a multifaceted and diverse environment in which flood risk differs considerably among the various cities/regencies across the watershed (Anna, 2021).Additionally, a large river passes through Surakarta (Absori et al., 2023) which makes the place prone to floods. A study conducted by

Hussain et al. (2021), pointed out that closeness to rivers, high rainfalls, elevation, and numerous socio-economic factors were the main determinants of the seriousness of flood risk. It should be known that increasing the level of awareness and understanding of flood risks by the local government (Cisternas et al., 2024), such as in Surakarta, is one way of increasing resilience while at the same time mitigating vulnerabilities (Muryani et al., 2021). More work must be done to design safety measures against floods that consider flood vulnerability features outlined in this research. Risk factors and vulnerabilities should be assessed when formulating relevant mitigation plans for flooding (Orru et al., 2023). By integrating components of physical, economic, and societal vulnerability within an interconnected system, there is a more extensive scope through which disaster impacts can be analysed, providing the direction for further improvement of mitigation strategies (Ward et al., 2012). Additionally, using GIS-based multi-criteria approaches can help determine flood risks among vulnerable areas to favour mitigation choices and resource distribution (Chakraborty et al., 2023).

Using spatial data can benefit decision-makers in designing mitigation plans precisely (Bakhtiari et al., 2024; Rezvani et al., 2023). For targeted mitigation measures, creation purposes like geographical location or attributes may identify at-risk areas (Liu & Li, 2016; Tellman et al., 2020). Concerning social aspects, this study looks into urbanization and population density levels. This work has added new dimensions to our understanding of flood vulnerability dynamics, especially in the Upper Solo basin, which helps us think about what we can face here. Therefore, it strengthens the use of GIS and remote sensing data, especially OASD to analyse flood risk. Determining where the danger lies encourages focused and efficacious efforts to address flooding problems (Chakraborty et al., 2023).

On the contrary, some limitations existed during the study. For example, long-term climatic change variables and fast-growing urbanization characteristics were not fully integrated in designing the risk model formulation. Therefore, future flood estimates should include hydrological data and other factors to maintain accuracy. However, these results come with limitations. Changes in climate over several decades or the rapid expansion of urban areas within the Upper Solo basin may not have been considered by this risk model (Marhaento et al., 2021). Information constraints or inadequate integration of non-hydrological variables could lead to less accurate forecasts of forthcoming flood risks. Besides, there has been an argument that risk maps alone might not properly illustrate susceptible regions unless they undergo supplementary validation processes. In any given research area, the social vulnerability of local populations is a crucial consideration that would require identifying probable locations to inform mitigation strategies. Consequently, a GIS-based methodology is useful because it helps us create flood risk maps needed for targeted interventions. After all, they show certain areas where more resources should be directed. The high-risk results for Surakarta substantiate the necessity for evidence-based mitigation actions to enhance the area's resilience against future flooding.

Moreover, Surakarta is situated next to a notable river; hence, it is at risk of flooding. The study by Hussain et al. (2021) underscored the role of the proximity of rivers, high precipitation levels, relief levels, and many socio-economic factors in determining a location's criticality. Realizing that people's knowledge about places like Surakarta, prone to floods, and their understanding of river inundation risks are essential to increase the population resilience and reduce vulnerabilities, as Muryani et al. (2021) indicate. It is further evident from research findings that more effort is needed to develop flood safety measures suited to the characteristics associated with flood vulnerability identified here. If we wish to protect our cities from going under, we must know what puts them there and what makes them vulnerable. The integration of physical, economic, and societal vulnerability components results in cohesive framework that enhances disaster impact analysis, thereby offering more than adequate guidance for mitigation strategies (Ward et al., 2012). In addition, GIS-enabled multi-criteria approaches can quantify flood risks within exposed zones, thereby giving preference to appropriate mitigation over available resources (Chakraborty et al., 2023).

High-risk regions' geographical attributes are very important in designing custom-tailored mitigation plans. This work's urban dimension hinged on levels of urbanization and population density. For example, in the Upper Solo watershed, this study provides a new perspective on the risk to floods among different populations thus guiding risk understanding. Therefore, this brings out the importance of detailed regional spatial analysis

using GIS data and remote sensing techniques. Identification of potential danger spots is thus supportive of specific and efficient strategies to counteract flooding (Chakraborty et al., 2023). Additionally, the historical data available serves as an extra reassurance for these conclusions.

4. Conclusion

This study uses OASD to build a GIS-based flood risk model based on population, urbanization levels, and various physical factors. Flood risk assessment in the Upper Solo River watershed has been successfully achieved using remote sensing data and geographic information systems. The results suggest that specific areas, namely Wonogiri, Karanganyar, and Boyolali, exhibit a lower risk of floods. Conversely, Sukoharjo, Surakarta, and certain parts of Karanganyar have an elevated risk, with Surakarta being the highest. The research highlights the need to incorporate physical and rural-urban attributes when evaluating flood risk, offering significant perspectives for formulating efficient approaches to preventing catastrophic events. The integrated methodology, which combines GIS technology with an analysis of physical and social factors, highlights the interconnectedness of natural and human elements in shaping the probability of floods. The research findings significantly contribute to understanding the specific geographical area and to the broader scholarly debate on mitigating catastrophic risks. The possible application of the research methodologies and results to comparable locations further increases the global importance and impact of the research.

The research on flood risk models has several limitations, mainly limited field validation. The model may not be sensitive to future factors like climate change, accelerating extreme rainfall patterns, and rapid land development in urban areas. Additionally, remote sensing data and GIS may not reflect actual field conditions fully. Future research should consider long-term climate change scenarios, updated high-resolution data, population growth, and land use change to produce more accurate flood risk projections. A collaborative approach involving field data and hydrological modelling based on climate data could improve the validity of the findings. Additionally, risk mapping at the micro or neighbourhood level could help develop more targeted mitigation strategies for local-scale implementation.

The study recommends flood mitigation strategies in the study area, including developing green infrastructure, sustainable drainage systems, and increased collaboration with the private sector. Green infrastructure, such as urban forests and infiltration parks, can reduce flooding impact and increase groundwater absorption. Sustainable drainage systems optimize water management and reduce surface water flow. Flood risk zoning should be implemented throughout the watershed, dividing areas based on vulnerability and potential flooding. Development and spatial planning regulations should be strengthened to align with flood mitigation efforts. Local governments should tighten building permits in flood-prone areas and require flood-resistant designs for new construction in high-risk areas. Community participation in flood risk management programs is crucial. Utilizing remote sensing technology and GIS can help predict potential flooding risks more accurately and support risk-based spatial planning. Capacity building of local governments and institutions is essential for supporting flood mitigation strategies, including training technical staff, strengthening coordination, and increasing disaster mitigation budgets.

5. Acknowledgments

The authors gratefully acknowledge Dirjend DIKTI, Kemendikbud for funding the research through the PFR Scheme, grant number 108/E5/PG.02.00.PL/2024, 007 /LL6/PB/AL.04/2024, 196.28/A.3-III/LRI/VI/2024.

6. References

Absori, A., Hernanda, T., Fitriciada, A., Wardiono, K., & Budiono, A. (2023). Analysis Of The Issues On Bengawan Solo River Basin Management Policies. *WSEAS Transactions on Environment and Development*, *19*, 25–32. [Crossref]

Amin, M. B. Al, Ilmiaty, R. S., & Marlina, A. (2020). Flood Hazard Mapping in Residential Area Using Hydrodynamic Model HEC-RAS 5.0. *Geoplanning: Journal of Geomatics and Planning*, *7*(1), 25–36. [Crossref]

Anna, A. N. (2021). Spatial Modelling of Local Flooding for Hazard Mitigation in Surakarta, Indonesia. *International Journal of GEOMATE*, *21*(87), 145–152. [Crossref]

Ayenew, W. A., & Kebede, H. A. (2023). GIS and remote sensing based flood risk assessment and mapping: The case of Dikala Watershed in Kobo Woreda Amhara Region, Ethiopia. *Environmental and Sustainability Indicators*, *18*, 100243. [Crossref]

Bakhtiari, V., Piadeh, F., Chen, A. S., & Behzadian, K. (2024). Stakeholder analysis in the application of cutting-edge digital visualisation technologies for urban flood risk management: A critical review. *Expert Systems with Applications*, *236*, 121426. [Crossref]

Biswajeet, P., & Mardiana, S. (2009). Flood hazrad assessment for cloud prone rainy areas in a typical tropical environment. *Disaster Advances*, *2*(2), 7–15.

Chagas, V. B. P., Chaffe, P. L. B., & Blöschl, G. (2022). Climate and land management accelerate the Brazilian water cycle. *Nature Communications*, *13*(1), 5136. [Crossref]

Chakraborty, L., Thistlethwaite, J., Scott, D., Henstra, D., Minano, A., & Rus, H. (2023). Assessing social vulnerability and identifying spatial hotspots of flood risk to inform socially just flood management policy. *Risk Analysis*, *43*(5), 1058–1078. [Crossref]

Chen, A. S., Evans, B., Djordjević, S., & Savić, D. A. (2012). Multi-layered coarse grid modelling in 2D urban flood simulations. *Journal of Hydrology*, *470–471*, 1–11. [Crossref]

Cisternas, P. C., Cifuentes, L. A., Bronfman, N. C., & Repetto, P. B. (2024). The influence of risk awareness and government trust on risk perception and preparedness for natural hazards. *Risk Analysis*, *44*(2), 333–348. [Crossref]

Curebal, I., Efe, R., Ozdemir, H., Soykan, A., & Sönmez, S. (2016). GIS-based approach for flood analysis: case study of Keçidere flash flood event (Turkey). *Geocarto International*, *31*(4), 355–366. [Crossref]

Damayanti, S. (2011). *Resilience for the 2007 flood event, using community knowledge: A Case in Part of Sukoharjo Regency, Indonesia*. University of Twente.

Diriba, D., Takele, T., Karuppannan, S., & Husein, M. (2024). Flood hazard analysis and risk assessment using remote sensing, GIS, and AHP techniques: a case study of the Gidabo Watershed, main Ethiopian Rift, Ethiopia. *Geomatics, Natural Hazards and Risk*, *15*(1), 2361813. [Crossref]

Earth Engine Data Catalog. (2023). *GHS-SMOD R2023A - Global Human Settlement Layers (1975-2030) | Earth Engine Data Catalog*. https://developers.google.com/earth-engine/datasets/catalog/JRC_GHSL_P2023A_GHS_SMOD

Elkhrachy, I. (2015). Flash Flood Hazard Mapping Using Satellite Images and GIS Tools: A case study of Najran City, Kingdom of Saudi Arabia (KSA). *The Egyptian Journal of Remote Sensing and Space Science*, *18*(2), 261–278. [Crossref]

European Commission. (2023). *Global Human Settlement GHSL Data and tools overview European Commission*. https://ghsl.jrc.ec.europa.eu/dataToolsOverview.php

Faisal, B. M. R., & Hayakawa, Y. S. (2023). Geomorphometric characterization and sediment connectivity of the middle Brahmaputra River basin. *Geomorphology*, *429*, 108665. [Crossref]

Fathimah, L., & Dahroni, D. (2014). *Tingkat Pengetahuan Siswa Kelas X Dalam Mitigasi Bencana Banjir Di SMA Islam 1 Surakarta*. Universitas Muhammadiyah Surakarta.

Ghimire, B., Chen, A. S., Guidolin, M., Keedwell, E. C., Djordjević, S., & Savić, D. A. (2013). Formulation of a fast 2D urban pluvial flood model using a cellular automata approach. *Journal of Hydroinformatics*, *15*(3), 676–686. [Crossref]

Greene, R. G., & Cruise, J. F. (1995). Urban Watershed Modeling Using Geographic Information System. *Journal of Water Resources Planning and Management*, *121*(4), 318–325. [Crossref]

Gunawan. (2009). *Studi banjir Bengawan Solo 2007 untuk peningkatan kinerja mitigasi bencana banjir: Studi kasus pada anak-anak Sungai Bengawan Solo antara Bendungan Colo di Sukoharjo dan Jurug di Surakarta*. https://etd.repository.ugm.ac.id/home/detail_pencarian/41549

Haq, M., Akhtar, M., Muhammad, S., Paras, S., & Rahmatullah, J. (2012). Techniques of Remote Sensing and GIS for flood monitoring and damage assessment: A case study of Sindh province, Pakistan. *The Egyptian Journal of Remote Sensing and Space Science*, *15*(2), 135–141. [Crossref]

Hussain, M., Tayyab, M., Zhang, J., Shah, A. A., Ullah, K., Mehmood, U., & Al-Shaibah, B. (2021). GIS-Based Multi-Criteria Approach for Flood Vulnerability Assessment and Mapping in District Shangla: Khyber Pakhtunkhwa, Pakistan. *Sustainability*, *13*(6), 3126. [Crossref]

Islam, M. D. M., & Sado, K. (2000). Development of flood hazard maps of Bangladesh using NOAA-AVHRR images with GIS. *Hydrological Sciences Journal*, *45*(3), 337–355. [Crossref]

Jamali, B., Löwe, R., Bach, P. M., Urich, C., Arnbjerg-Nielsen, K., & Deletic, A. (2018). A rapid urban flood inundation and damage assessment model. Journal of Hydrology, *564*, 1085–1098. [Crossref]

Jumadi, Carver, S., & Quincey, D. (2016). ABM and GIS-based multi-scenarios volcanic evacuation modelling of Merapi. *AIP Conference Proceedings*, *1730*(1), 050005. [Crossref]

Jumadi, J., Novita, S. D., Umrotun, U., Musiyam, M., Nurmantyo, C., Muhammad, S. F., & Ibrahim, M. H. (2024). Remote Sensing and GIS-Driven Model for Flood Susceptibility Assessment in the Upper Solo River Watershed. *Geographia Technica*, *19*(2/2024), 33–45. [Crossref]

Komolafe, A. A., Awe, B. S., Olorunfemi, I. E., & Oguntunde, P. G. (2020). Modelling flood-prone area and vulnerability using integration of multi-criteria analysis and HAND model in the Ogun River Basin, Nigeria. *Hydrological Sciences Journal*, *65*(10), 1766–1783. [Crossref]

Li, Y., Gao, J., Yin, J., Liu, L., Zhang, C., & Wu, S. (2024). Flood Risk Assessment of Areas under Urbanization in Chongqing, China, by Integrating Multi-Models. *Remote Sensing*, *16*(2), 219. [Crossref]

Liu, D., & Li, Y. (2016). Social vulnerability of rural households to flood hazards in western mountainous regions of Henan province, China. *Natural Hazards and Earth System Sciences*, *16*(5), 1123–1134. [Crossref]

Marhaento, H., Booij, M. J., & Ahmed, N. (2021). Quantifying relative contribution of land use change and climate change to streamflow alteration in the Bengawan Solo River, Indonesia. *Hydrological Sciences Journal*, *66*(6), 1059–1068. [Crossref]

Melchiorri, M. (2022). The global human settlement layer sets a new standard for global urban data reporting with the urban centre database. *Frontiers in Environmental Science*, *10*, 1003862. [Crossref]

Mukherjee, F., & Singh, D. (2020). Detecting flood prone areas in Harris County: a GIS based analysis. *GeoJournal*, *85*(3), 647–663. [Crossref]

Muryani, C., Koesuma, S., & Yusup, Y. (2021). People Perception and Participation in Disaster Risk Reduction at Surakarta City, Central Java, Indonesia. *GeoEco*, *7*(1), 96–105.

Mustikaningrum, M., Widhatama, A. F., Widantara, K. W., Ibrohim, M., Hibatullah, M. F., Larasati, R. A. P., Utami, S., & Hadmoko, D. S. (2023). Multi-Hazard Analysis in Gunungkidul Regency Using Spatial Multi-Criteria Evaluation. *Forum Geografi*, *37*(1). [Crossref]

Nada, F. M. H., Nugroho, N. P., & Sofwa, N. B. M. (2023). Lake and Stream Buffer Zone Widths' Effects on Nutrient Export to Lake Rawapening, Central Java, Indonesia: A Simple Simulation Study. *Forum Geografi*, *37*(1). [Crossref]

Negese, A., Worku, D., Shitaye, A., & Getnet, H. (2022). Potential flood-prone area identification and mapping using GIS-based multi-criteria decision-making and analytical hierarchy process in Dega Damot district, northwestern Ethiopia. *Applied Water Science*, *12*(12), 255. [Crossref]

Orru, K., Klaos, M., Nero, K., Gabel, F., Hansson, S., & Nævestad, T.-O. (2023). Imagining and assessing future risks: A dynamic scenario-based social vulnerability analysis framework for disaster planning and response. *Journal of Contingencies and Crisis Management*, *31*(4), 995–1008.

Osman, S. A., & Das, J. (2023). GIS-based flood risk assessment using multi-criteria decision analysis of Shebelle River Basin in southern Somalia. *SN Applied Sciences*, *5*(5), 134. [Crossref]

Ozkan, S. P., & Tarhan, C. (2016). Detection of Flood Hazard in Urban Areas Using GIS: Izmir Case. *Procedia Technology*, *22*, 373–381. [Crossref]

Paudyal, G. N. (1996). An integrated GIS-numerical modelling system for advanced flood management. *Proceeding of the International Conference on Water Resources and Environment Research: Towards the 21st Century, Kyoto University, Japan*, *555–562*.

Pradhan, B., Shafiee, M., & Pirasteh, S. (2009). Maximum flood prone area mapping using RADARSAT images and GIS: Kelantan river basin. *International Journal of Geoinformatics*, *5*(2).

Purwanto, A., Andrasmoro, D., Eviliyanto, E., Rustam, R., Ibrahim, M. H., & Rohman, A. (2023). Validating the GIS-based Flood Susceptibility Model Using Synthetic Aperture Radar (SAR) Data in Sengah Temila Watershed, Landak Regency, Indonesia. *Forum Geografi*, *36*(2), 185–201. [Crossref]

Purwitaningsih, S., Pamungkas, A., Setyasa, P. T., Pamungkas, R. P., Alfian, A. R., & Irawan, S. A. R. (2020). Flood-reduction scenario based on land use in Kedurus river basin using SWAT hydrology model. *Geoplanning: Journal of Geomatics and Planning*, *7*(2), 87–94. [Crossref]

Rana, S. M. S., Habib, S. A., Sharifee, M. N. H., Sultana, N., & Rahman, S. H. (2024). Flood risk mapping of the flood-prone Rangpur division of Bangladesh using remote sensing and multi-criteria analysis. *Natural Hazards Research*, *4*(1), 20–31. [Crossref]

Rezvani, S. M., Falcão, M. J., Komljenovic, D., & de Almeida, N. M. (2023). A Systematic Literature Review on Urban Resilience Enabled with Asset and Disaster Risk Management Approaches and GIS-Based Decision Support Tools. *Applied Sciences*, *13*(4), 2223. [Crossref]

Rincón, D., Khan, U. T., & Armenakis, C. (2018). Flood Risk Mapping Using GIS and Multi-Criteria Analysis: A Greater Toronto Area Case Study. *Geosciences*, *8*(8), 275. [Crossref]

Samarasinghea, S., Nandalalb, H. K., Weliwitiyac, D. P., Fowzed, J. S. M., Hazarikad, M. K., & Samarakoond, L. (2010). Application of remote sensing and GIS for flood risk analysis: a case study at Kalu-Ganga River, Sri Lanka. *International Archives of the Photogrammetry, Remote Sensing and Spatial Information Science*, *38*(8), 110–115.

Samphantharak, K. (2019). Natural Disaster and Economic Development in Southeast Asia. *SSRN Electronic Journal*. [Crossref]

Saputra, A., Sigit, A. A., Priyana, Y., Abror, A. M., Sari, A. N. L., & Nursetiyani, O. (2022). A Low-Cost Drone Mapping and Simple Participatory GIS to Support The Urban Flood Modelling. *Geographia Technica*, *17*(2).

Sar, N., Chatterjee, S., & Das Adhikari, M. (2015). Integrated remote sensing and GIS based spatial modelling through analytical hierarchy process (AHP) for water logging hazard, vulnerability and risk assessment in Keleghai river basin, India. *Modeling Earth Systems and Environment*, *1*(4), 31. [Crossref]

Sarmah, T., Das, S., Narendr, A., & Aithal, B. H. (2020). Assessing human vulnerability to urban flood hazard using the analytic hierarchy process and geographic information system. *International Journal of Disaster Risk Reduction*, *50*, 101659. [Crossref]

Sejati, A. W., Putri, S. N. A. K., Rahayu, S., Buchori, I., Rahayu, K., Wiratmaja, I. G. A. M. A., Muzaki, A., & Basuki, Y. (2023). Flood hazard risk assessment based on multi-criteria spatial analysis GIS as input for spatial planning policies in Tegal Regency, Indonesia. *Geographica Pannonica*, *27*(1), 50–68. [Crossref]

Skilodimou, H. D., Bathrellos, G. D., Chousianitis, K., Youssef, A. M., & Pradhan, B. (2019). Multi-hazard assessment modeling via multi-criteria analysis and GIS: a case study. *Environmental Earth Sciences*, *78*(2), 47. [Crossref]

Sofia, G. (2020). Combining geomorphometry, feature extraction techniques and Earth-surface processes research: The way forward. *Geomorphology*, *355*, 107055. [Crossref]

Susetyo, C. (2008). *Urban flood management in Surabaya City: anticipating changes in the Brantas River system.*

Tehrany, M. S., Shabani, F., Neamah Jebur, M., Hong, H., Chen, W., & Xie, X. (2017). GIS-based spatial prediction of flood prone areas using standalone frequency ratio, logistic regression, weight of evidence and their ensemble techniques. *Geomatics, Natural Hazards and Risk*, *8*(2), 1538–1561. [Crossref]

Tellman, B., Schank, C., Schwarz, B., Howe, P. D., & de Sherbinin, A. (2020). Using Disaster Outcomes to Validate Components of Social Vulnerability to Floods: Flood Deaths and Property Damage across the USA. *Sustainability*, *12*(15), 6006. [Crossref]

UNISDR. (2004). *Living with risk: A global review of disaster reduction initiatives.*

Ward, S. M., Emrich, C. T., Ash, K., & Schumann, R. (2012). Research-Based Decision Support in Hazard Mitigation: Louisiana Northshore Flood and Hurricane Protection. *Risk, Hazards & Crisis in Public Policy*, *3*(3), 38–68. [Crossref]

Xiong, L., Li, S., Tang, G., & Strobl, J. (2022). Geomorphometry and terrain analysis: data, methods, platforms and applications. *Earth-Science Reviews*, *233*, 104191. [Crossref]

Zein, M. (2010). *A community-based approach to flood hazard and vulnerability assessment in flood prone areas; A case study in Kelurahan Sewu, Surakarta City-Indonesia.* University of Twente.

Zhou, Q., Su, J., Arnbjerg-Nielsen, K., Ren, Y., Luo, J., Ye, Z., & Feng, J. (2021). A GIS-Based Hydrological Modeling Approach for Rapid Urban Flood Hazard Assessment. *Water*, *13*(11), 1483. [Crossref]